

Review

Design, Synthesis and Molecular Modeling Study of Radiotracers Based on Tacrine and Its Derivatives for Study on Alzheimer's Disease and Its Early Diagnosis

Przemysław Koźmiński *  and Ewa Gniazdowska * 

Centre of Radiochemistry and Nuclear Chemistry, Institute of Nuclear Chemistry and Technology,
03-195 Warsaw, Poland

* Correspondence: p.kozminski@ichtj.waw.pl (P.K.); e.gniazdowska@ichtj.waw.pl (E.G.)

Abstract: From 1993 to 2013, tacrine was an approved drug for Alzheimer's disease. Due to its strong inhibitory properties towards cholinesterase, tacrine causes an increase in the level of the neurotransmitter acetylcholine in the cholinergic system of the central nervous system. This work presents a review of articles in which tacrine or its derivatives labeled with the radionuclides ^3H , ^{11}C , ^{14}C , ^{123}I , $^{99\text{m}}\text{Tc}$ and ^{68}Ga were used as vectors in radiotracers dedicated to the diagnosis of Alzheimer's disease. The possibility of clinical applications of the obtained radiopreparations was assessed by analyzing their physicochemical properties, ability to cross the blood–brain barrier and the level of uptake in the brain. Based on these data, it was shown that radiopreparations based on the tacrine molecule or its very close analogues retain the ability to cross the blood–brain barrier, while radiopreparations containing a more modified tacrine molecule (connected via a linker to a radionuclide chelator) lose this ability. This is probably the result of the addition of a chelator, which significantly increases the size of the radiopreparation and reduces its lipophilicity. Computer docking studies of tacrine derivatives and/or radiopreparations showed how these compounds bind to the active sites of acetyl- and butyrylcholinesterase.

Keywords: Alzheimer's disease; tacrine; radiopharmaceuticals; molecular modeling; PET; SPECT



Citation: Koźmiński, P.;

Gniazdowska, E. Design, Synthesis and Molecular Modeling Study of Radiotracers Based on Tacrine and Its Derivatives for Study on Alzheimer's Disease and Its Early Diagnosis. *Appl. Sci.* **2024**, *14*, 2827. <https://doi.org/10.3390/app14072827>

Academic Editor: Qi-Huang Zheng

Received: 30 January 2024

Revised: 19 March 2024

Accepted: 25 March 2024

Published: 27 March 2024



Copyright: © 2024 by the authors. Licensee MDPI, Basel, Switzerland. This article is an open access article distributed under the terms and conditions of the Creative Commons Attribution (CC BY) license (<https://creativecommons.org/licenses/by/4.0/>).

1. Introduction

Alzheimer's disease (AD) is a progressive central nervous system (CNS) disease leading to the loss of cognitive abilities, the initial symptoms of which are often attributed to the normal aging process [1–3]. The initial stage of the disease may last for many years and is often latent. In the final stage of the disease, the patient is unable to perform basic everyday activities. Alzheimer's disease cannot be cured. Nevertheless, early symptomatic treatment helps alleviate the symptoms and delay the progression of the disease. However, this requires an early diagnosis, which is usually unattainable due to the long latent period of the disease and the lack of morphological symptoms. Such pathophysiological symptoms in everyday functioning, such as dementia, loss of memory and orientation and loss of daily physical activities, which are often similar to those of other diseases, are already visible at the stage of very advanced AD. The causes of Alzheimer's disease are not clearly defined. Many risk factors, both environmental and genetic, are considered here. These may be, for example, a head injury, clinical depression, high blood pressure [3] or a genetic factor [4,5]. In the course of Alzheimer's disease, increased amounts of beta-amyloid ($\text{A}\beta$) accumulate in the brain, which can accumulate extracellularly in the form of amyloid plaques and tau proteins or intracellularly in the form of neurofibrillary tangles—both of these phenomena cause impairment of neuronal transmission, leading to the loss of proper brain function [6]. AD cannot be cured, and already existing pathophysiological symptoms cannot be reversed. However, it is possible to slow down the course of this disease and reduce its cognitive symptoms. An early pathophysiological feature of the mild to moderate stages of AD is

loss of memory and cognitive function, caused by a deficiency of the neurotransmitter acetylcholine (ACh). ACh deficiency results from its hydrolysis, induced by the enzyme acetylcholinesterase (AChE), and leads to the selective loss of cholinergic neurons in the cerebral cortex, basal ganglia and hippocampus [7]. The two main therapeutic strategies in AD are influencing the processing of amyloid precursor protein (APP) and slowing the decline of neuronal degeneration and improving cholinergic neurotransmission [1,7–10]. As therapeutic agents in the mild and moderate stages of Alzheimer’s disease, AChE inhibitors, e.g., tacrine, rivastigmine, galantamine and donepezil, have been used [11–14]. One of the known and tested inhibitors is tacrine (1,2,3,4-tetrahydro-9-amino acridine, THA)—the active substance of the drug Cognex [15,16], approved in 1993 by the US Food and Drug Administration (FDA) for use in treating the symptoms of AD. The therapeutic effect of THA is achieved by reversible binding to AChE and its inactivation, which results in an increase in the concentration of ACh at cholinergic synapses, thanks to which a greater number of cholinergic neurons remain intact, and the progression of the disease is slowed down [10,12,17,18]. Tacrine is characterized by high biological activity towards AChE, but unfortunately, it causes a number of common side effects (nausea, indigestion, vomiting, anorexia, abdominal pain, diarrhea, skin rash) and a high risk of liver damage, especially when using large doses of the drug [11–14,19]. In 2013, it was withdrawn due to hepatotoxicity and cardiovascular problems occurring in patients.

Nevertheless, both tacrine and its derivatives have been used as biologically active molecules in potential radiopharmaceuticals dedicated to the early diagnosis of Alzheimer’s disease [1]. Diagnostic radiopharmaceuticals are compounds that use a biologically active molecule as a vector and contain a diagnostic radionuclide emitting gamma or beta plus radiation. They are administered to the patient in nanomolar amounts, so they do not cause any morphological changes in the body. At the same time, registration of the emitted radiation allows for the precise location of the radiopharmaceutical in the patient’s body and thus the location of the disease lesion.

In the presented review, we collected and discussed data on radioactively labeled tacrine and its derivatives indicated to the early diagnosis of Alzheimer’s disease. Specific consideration has been placed on the role of computational molecular modeling in the visualization of the interaction of tacrine with cholinesterase.

2. Radiolabeled Tacrine and Its Derivatives Used in Alzheimer’s Disease

There are many papers on tacrine and its use in treating the symptoms of Alzheimer’s disease but only a dozen papers on the use of tacrine and its derivatives as a vector in described radiotracers.

2.1. Radiotracers Based on Tacrine

One of the first tacrine-based radiopreparations was the [9-¹⁴C]tacrine radiotracer (Figure 1A) [20,21]. The authors examined the distribution of this radiotracer in the rat body after both intravenous and oral administration using a quantitative whole-body autoradiographic method [20]. Based on the results obtained, the authors concluded that, in both cases, [¹⁴C]tacrine ([¹⁴C]THA) crosses the blood–brain barrier; the biodistribution of the radiotracer is similar, although after oral administration, the absorption of the radiotracer persists in the organs noticeably longer. Due to the potential use of ([¹⁴C]THA) in the diagnosis of neurological diseases, the authors examined the regional distribution of the radiotracer in the brain—the highest levels of radioactivity were detected in the cortex, hippocampus, cerebellum and striatum. Analyzing the distribution of the radiotracer in individual parts of the brain, the authors found that it did not correlate consistently with the distribution of acetylcholinesterase (AChE), which may suggest that the effect of tacrine in the treatment of senile dementia may occur in a way other than by inhibiting the enzyme. Based on the high level of activity detected in the kidneys and ureters, the authors also concluded that the radiotracer is excreted primarily in the urine, although they

also noted that there are indications of excretion of the radiotracer and its metabolites into the intestines.

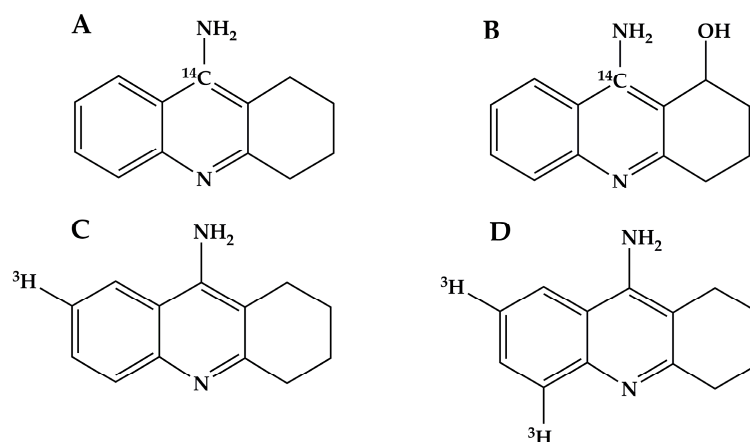


Figure 1. Radiotracers based on tacrine: (A) [9-¹⁴C]tacrine [20,21]; (B) [9-¹⁴C]1-OH-THA [21]; (C) [7-³H]tacrine [22,23]; (D) [5,7-³H]tacrine [23].

Further research by McNally et al. on the application of the radiotracer [9-¹⁴C]tacrine (Figure 1A) in the study of THA distribution in the brain is presented in [21]. Using oral administration (by oral gavage) and single or multiple (twice daily for 3 days) doses (SD or MD, respectively), the authors performed *in vivo* studies of the distribution of [9-¹⁴C]THA and its main metabolite [9-¹⁴C]1-OH-tacrine ([9-¹⁴C]1-OH-THA, Figure 1B) in rats. At selected time intervals, ranging from 0.5 h to 96 h, they examined the level of radioactivity in blood, plasma, the heart, the lungs, the kidneys, the liver, the pancreas and various brain regions (brainstem, cerebellum, cortex, hippocampus, striatum and thalamus) using the autoradiography method. The authors also performed *in vitro* studies of the process of tacrine metabolism in the brain. The rat brain homogenate was incubated with the [9-¹⁴C]THA radiotracer and its metabolite [9-¹⁴C]1-OH-THA. Then, after the incubation, the products of tacrine metabolism were identified using the HPLC method in specially prepared samples. For this purpose, various products of tacrine metabolism ([9-¹⁴C]1-OH-THA, [9-¹⁴C]2-OH-THA and [9-¹⁴C]4-OH-THA) and their reference compounds (1-OH-THA, 2-OH-THA and 4-OH-THA) were previously characterized by HPLC. Based on the results obtained, McNally et al. drew a number of conclusions. They found that, for both doses used (SD and MD), the distribution of [9-¹⁴C]THA in the brain was similar, although in the case of MD, the radioactivity levels in the tested organs were visibly higher. After oral administration of [9-¹⁴C]THA, the radiotracer penetrates very quickly into the brain and accumulates in the cortex and hippocampus, i.e., in the areas responsible for the cognitive functions of the brain. *In vitro* studies of tacrine metabolism in the brain performed using rat brain homogenate showed that this process practically does not occur in the brain and that metabolite [9-¹⁴C]1-OH-THA has a very limited ability to cross the blood–brain barrier. This difference in the ability to cross the blood–brain barrier correlates well with the log *p* values calculated by the authors for THA and its metabolite 1-OH-THA (3.30 and 1.66, respectively). The lack of transformation of tacrine into its metabolites in the brain and low ability of metabolites to cross the blood–brain barrier correlate perfectly with (observed in radioautographic studies in rats) a slight accumulation of [9-¹⁴C]1-OH-THA in the brain and a high level of [9-¹⁴C]1-OH-THA in the blood, which explains the significantly higher brain-to-plasma ratio determined for tacrine than for its 1-OH-THA metabolite. The results of the experiments conducted by the authors also indicate that the transport of THA and its metabolites to the brain tissue takes place through a simple passive process, and the excretion of these compounds occurs through the biliary and urinary tracts.

Tritium-labelled tacrine, [7-³H]tacrine ([³H]THA), a very close analogue of tacrine, custom synthesized from 7-bromo-9-amino-1,2,3,4-tetrahydroacridine, Figure 1C), was used in the study by Mena et al. to locate tacrine binding sites in the rat brain [22]. Using P2

membrane fractions prepared from rat brain, Mena and Desai performed a number of tests: AChE enzymatic test, localization of [^3H]THA binding sites, kinetic parameters of [^3H]THA binding using various concentrations of inactive THA and the ability of THA to inhibit AChE. In order to be able to compare the results obtained, experimental conditions (buffer, pH, concentration of the tested compound) as similar as possible were used in all studies. Based on the results obtained, the authors concluded that [^3H]THA binds to the membrane almost rapidly but in a reversible manner—adding an inactive ligand completely removed [^3H]THA from the membrane. They also showed that the binding of [^3H]THA in the rat brain is not blocked by a number of other neurotransmitters/neuromodulators, so the binding site of [^3H]THA is different from the sites of action (sites of receptors) of these compounds. Moreover, their research (autoradiography) also showed that [^3H]THA binding sites are not located together with the activity of acetylcholine (and other acetylcholinesterase inhibitors); therefore, it can be concluded that the clinical effect of THA may also result from an action other than through the cholinergic neuronal system.

The procedure for the synthesis of tritium-labeled tacrine was described by Egan et al. [23]. The authors synthesized two radiopreparations, [7- ^3H]tacrine (Figure 1C) and [5,7- ^3H]tacrine (Figure 1D), using the catalytic tritium dehalogenation of 7-bromo-tacrine and 5,7-dibromo-tacrine compounds, respectively. The products of the individual stages of synthesis were analyzed using the proton and tritium NMR method and TLC and HPLC methods equipped with UV and/or liquid scintillation detectors.

In 2007, Jogani et al. presented the results of studies on the intravenous and intranasal administration of tacrine labeled with technetium-99m [24]. The labeling reaction was performed directly using a solution of tacrine in propylene glycol, reducing agent SnCl_2 and pertechnetate solution [$^{99\text{m}}\text{Tc}$]TcO $_4^-$ (eluate from the $^{99}\text{Mo}/^{99\text{m}}\text{Tc}$ generator). The authors demonstrated the stability of the radiopreparation in normal saline solution and in mouse serum as well as in a challenge experiment with DTPA (diethylenetriamine pentaacetic acid). Unfortunately, the obtained radiopreparation [$^{99\text{m}}\text{Tc}$]Tacrine solution ([$^{99\text{m}}\text{Tc}$]Tc-TS) was tested only by thin-layer chromatography (TLC) using silica gel-coated fiberglass sheets as a stationary phase and two different mobile phases: acetone and pyridine:acetic acid:water (3:5:1.5, *v/v*). The structure of [$^{99\text{m}}\text{Tc}$]Tc-TS is also unknown. The paper presents the results of biodistribution studies in mice and γ -scintigraphy imaging studies (performed using single photon emission computerized tomography, SPECT) in rabbits. In both studies, intravenous (IV) and intranasal (IN) administrations of [$^{99\text{m}}\text{Tc}$]Tc-TS were used. The results of these studies showed that the tacrine concentration in the brain after intranasal administration was significantly higher than after intravenous administration. The authors concluded that nasal-to-brain administration of tacrine may provide an alternative route to the currently used oral route, which is limited by tacrine's low bioavailability and pronounced side effects.

Jogani et al. continued to study tacrine delivery to the brain via the nasal route using other tacrine formulations [25]. It is known that, in nasal drug administration, the application of microemulsion and mucoadhesive agent, due to the small size of the globules and their lipophilicity, effectively improves the delivery process of a drug by increasing the retention of formulations at the absorption site. The authors prepared and characterized tacrine solution (TS), tacrine microemulsion (TME) and tacrine mucoadhesive microemulsion (TMME) and assessed their pharmacokinetic and pharmacodynamic properties in the process of tacrine delivery to the brain. Then, similarly to previous studies [24], all three tacrine formulations were labeled with $^{99\text{m}}\text{Tc}$ radionuclide to obtain the radiopreparations [$^{99\text{m}}\text{Tc}$]Tc-TS, [$^{99\text{m}}\text{Tc}$]Tc-TME and [$^{99\text{m}}\text{Tc}$]Tc-TMME. As before, the stability of all three radiotracers was tested in normal saline solution and in mouse serum as well as in a challenge experiment with DTPA. Using different routes of administration (intranasal (IN) and intravenous (IV)) and all three radiotracers, the authors performed biodistribution studies in mice and γ -scintigraphy imaging studies in rabbits. Analyzing the results obtained in all studies (for TS, TME, TMME, [$^{99\text{m}}\text{Tc}$]Tc-TS, [$^{99\text{m}}\text{Tc}$]Tc-TME and [$^{99\text{m}}\text{Tc}$]Tc-TMME and IN or IV administration), the authors showed that, in the case of intranasal administration, the

accumulation of a given tacrine formulation (TS, TME, TMME, [^{99m}Tc]Tc-TS, [^{99m}Tc]Tc-TME and [^{99m}Tc]Tc-TMME) in the brain and the brain/blood ratio was higher than in the case of intravenous administration. They also showed that the most efficient transport of tacrine to the brain was observed in the case of TMME-based preparations, followed by TME-based preparations, and the lowest was observed in the case of TS-based preparations. The results of the study by Jogani et al. suggest that the intranasal administration of an appropriate tacrine formulation may minimize gastrointestinal and hepatic side effects and may play an important role in the treatment of patients with Alzheimer's disease.

Concise information concerning radiotracers based on tacrine is presented in Table 1.

Table 1. Radiotracers based on tacrine.

Tacrine-Based Radiotracers	Research Purpose and Conclusions	References
[9- ¹⁴ C]tacrine ([¹⁴ C]THA)	<p>Distribution of the radiopreparation in the rat body after both intravenous and oral administration, studies of the process of tacrine metabolism in the brain</p> <ul style="list-style-type: none"> • In both cases, [¹⁴C]THA crosses the blood–brain barrier; • Biodistribution of the radiotracer is similar, although after oral administration, the absorption of the radiotracer persists noticeably longer in the organs; • The highest levels of radioactivity were detected in the cortex, hippocampus, cerebellum and striatum; • The radiotracer is excreted mainly in the urine and partly through the intestines; • Tacrine metabolism practically does not occur in the brain; • The main metabolite of tacrine is [9-¹⁴C]1-OH-THA, and it has a very limited ability to cross the blood–brain barrier. 	[20,21]
[7- ³ H]tacrine ([³ H]THA)	<p>AChE enzymatic test, localization of [³H]THA binding sites in the rat brain, kinetic parameters of [³H]THA binding, ability of THA to inhibit AChE</p> <ul style="list-style-type: none"> • [³H]THA binds to the membrane almost rapidly but in a reversible manner; • Binding of [³H]THA in the rat brain is not blocked by a number of other neurotransmitters/neuromodulators, so the binding site of [³H]THA is different from the sites of action of these compounds; • [³H]THA binding sites are not located together with the activity of acetylcholine (and other acetylcholinesterase inhibitors), so it can be concluded that the clinical effect of THA may also result from an action other than through the cholinergic neuronal system. 	[22]
[7- ³ H]tacrine and [5,7- ³ H]tacrine	<p>Procedure for the synthesis of tritium-labeled tacrine, analysis of products using TLC, HPLC and NMR methods</p>	[23]
[^{99m} Tc]Tacrine solution ([^{99m} Tc]Tc-TS)	<p>Studies on the intravenous (IV) and intranasal (IN) administration of tacrine labeled with technetium-99m, biodistribution studies in mice</p> <ul style="list-style-type: none"> • The tacrine concentration in the brain after IN administration is significantly higher than after IV administration; • Nasal-to-brain administration of tacrine may provide an alternative route to the currently used oral route, which is limited by tacrine's low bioavailability and pronounced side effects. 	[24]
[^{99m} Tc]Tc-TS, [^{99m} Tc]Tc-TME, [^{99m} Tc]Tc-TMME	<p>Syntheses and characterization of tacrine solution (TS), tacrine microemulsion (TME) and tacrine mucoadhesive microemulsion (TMME) and assessment of their pharmacokinetic and pharmacodynamic properties in the process of tacrine delivery to the brain, radiolabeling of these tacrine formulations with ^{99m}Tc, biodistribution studies in mice after intravenous (IV) and intranasal (IN) administration</p> <ul style="list-style-type: none"> • In the case of IN administration, the accumulation of a given tacrine formulation in the brain and the brain/blood ratio are higher than in the case of IV administration; • The most efficient transport of tacrine to the brain was observed in the case of TMME-based preparations, followed by TME-based preparations, and the lowest was observed in the case of TS-based preparations • IN administration of an appropriate tacrine formulation may minimize gastrointestinal and hepatic side effects and may play an important role in the treatment of patients with AD 	[25]

2.2. Radiotracers Based on Tacrine Derivatives

Some of the first reports on radionuclide-labeled tacrine derivatives are the papers presenting 1,2,3,4-tetrahydro-9-methyl-amino acridine (N-methyl-THA, MTHA) labeled with ^{11}C radionuclide, synthesized by Bonnot et al. [26] and studied in vivo in non-human primates by Tavitian et al. [27] and in healthy human volunteers by Traykov et al. [28]. In vitro testing of tacrine (THA) and its N-methyl derivative MTHA showed that both compounds have very similar inhibitory properties towards acetylcholinesterase (AChE) [27]. The authors conducted a study of the distribution of the [methyl- ^{11}C]1,2,3,4-tetrahydro-9-methyl-amino acridine radiotracer ($[^{11}\text{C}]\text{MTHA}$, Figure 2A) in rats (radioactivity was measured in blood, plasma, the heart, the liver, the kidneys, the lungs, skeletal muscles and the brain (separately in the pons, cerebellum, colliculi, hypothalamus, hippocampus, striatum and anterior and posterior cortices)), and positron emission tomography (PET) imaging was performed on two male adult baboons. In these experiments (distribution study in rats and PET imaging in baboons), both $[^{11}\text{C}]\text{MTHA}$ radiotracer alone and $[^{11}\text{C}]\text{MTHA}$ radiotracer together with unlabeled THA administered simultaneously or 20 min before tracer injection were used. The results, in the case of using the $[^{11}\text{C}]\text{MTHA}$ radiopreparation and in the case of administering the $[^{11}\text{C}]\text{MTHA}$ radiopreparation and then unlabeled THA, showed significantly different amounts of radioactivity accumulated in the examined organs, significantly lower in the case of using unlabeled THA in the experiment, e.g., radioactivity accumulated in all brain regions studied in the case of coinjection of THA together with $[^{11}\text{C}]\text{MTHA}$ was 40–50% lower. This allows for us to conclude that these two molecules ($[^{11}\text{C}]\text{MTHA}$ and THA) compete for the same binding sites. Based on these results, the authors concluded that the $[^{11}\text{C}]\text{MTHA}$ radiotracer could be considered a promising PET ligand for studying THA binding in the brain.

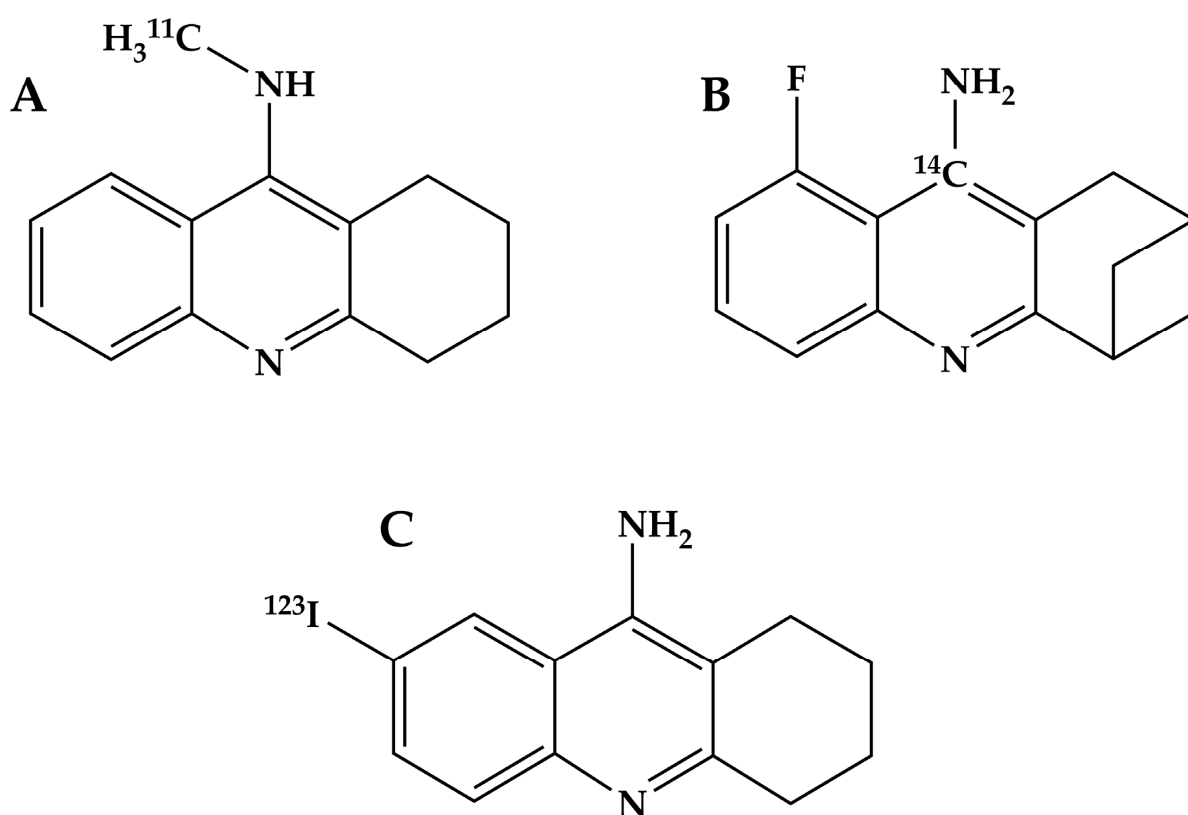


Figure 2. Radiotracers based on tacrine derivatives: (A) [methyl- ^{11}C]1,2,3,4-tetrahydro-9-methyl-amino acridine [26–28]; (B) 9-amino-8-fluoro-2,4-methane-1,2,3,4-[^{14}C]tetrahydroacridine [29]; (C) 7-[^{123}I]iodotacrine [30].

The first studies of the [^{11}C]MTHA radiotracer (Figure 2A) in position emission tomography (PET) imaging in healthy volunteers are presented in the publication by Traykov et al. [28]. The study involved four healthy men who had never been diagnosed with Alzheimer's disease or other chronic diseases. The [^{11}C]MTHA radiotracer was used in PET and magnetic resonance imaging (MRI) methods in order to obtain individual cerebral anatomy. At specific time intervals (up to 70 min after intravenous administration of the tracer), the authors determined the level of radioactivity in the blood and in the selected areas of the brain (white matter, putamen, thalamus, brainstem, cerebellum, cortex). The determined radioactivity in the brain was relatively high and amounted to approximately 6% of the administered dose. Radioactivity in the blood, after a rapid increase (approximately 1.5 min after administration) and then an equally rapid decline (approximately 5 min after administration), increased very slightly; this is related to the circulation of radiotracer metabolites ([^{11}C]1-hydroxy-MTHA) in the blood [21], which are, however, capable of crossing the blood–brain barrier to a significantly lesser extent than the administered radiotracer [21]. Traykov's study also showed that brain accumulation of the radiotracer [^{11}C]MTHA differs from the sites of action and/or sites of elevated AChE concentrations detected post-mortem in human brains. This allows for us to assume that the cerebral distribution of the [^{11}C]MTHA radiotracer in the human nervous system is not parallel with AChE, so the clinical effect of THA may also occur in a way other than through the cholinergic neuronal system, which has already been discussed in previous works [20,22].

Another radionuclide-labeled tacrine derivative is the radiopreparation based on the cholinesterase inhibitor 9-amino-8-fluoro-2,4-methane-1,2,3,4-tetrahydroacridine in which ^{14}C radionuclide is located in position 9 of the tetrahydroacridine ring (Figure 2B) [29]. Practically in every step of the synthesis of this radiotracer, the obtained intermediates were tested using many analytical methods (radio-thin layer chromatography (RTLC), radio-high performance liquid chromatography (RHPLC), infrared spectrum (IR), proton nuclear magnetic resonance (NMR) and mass spectrum (MS)). According to the authors' intention, this radiopreparation was to be used in metabolic studies, but due to the presence of a tacrine derivative and therapeutic radionuclide C-14, it could also be considered as a potential therapeutic radiopharmaceutical in Alzheimer's disease. However, this would also require physicochemical tests of the compound (lipophilicity, stability in body fluids and serum), which were not tested in this work.

Akula et al. developed a four-step synthesis procedure of 7-[^{123}I]iodotacrine ([^{123}I]7-I-THA, Figure 2C), a potential imaging agent for single photon emission computer tomography (SPECT), to map acetylcholinesterase (AChE) receptor sites in living organisms [30]. In each step of the synthesis of the [^{123}I]7-I-THA radiopreparation, the obtained intermediates were tested using analytical methods: melting points, elemental analysis and ^1H - and ^{13}C -NMR analyses. The radiochemical purity of the [^{123}I]7-I-THA radiopreparation was tested by thin-layer chromatography (TLC) using an aluminum silica gel plate and a chloroform/methanol mixture (4:1, *v/v*) as a developing solvent. However, there are no reports in the literature of further studies using this radiotracer.

In the years 2017–2022, several works were published in which the labeling of tacrine derivatives with the diagnostic radionuclides $^{99\text{m}}\text{Tc}$ and ^{68}Ga was presented. The procedures for synthesizing and testing the physicochemical properties of the tacrine derivatives used here were designed and described by Szymański et al. [31,32]. The structural modification of tacrine consisted of attaching to the amino group of tacrine an aliphatic hydrocarbon chain composed of $-(\text{CH}_2)_n-$ groups (where the number of carbon atoms *n* was from two to nine) and a bifunctional coupling agent (BFCA) capable of forming complexes with a given radionuclide. It was a series of compounds that differed only in the number of methylene groups (affecting the lipophilicity parameter of the compound) between tetrahydroacridine and the radionuclide complexing moiety.

The work by Gniazdowska et al. presents the syntheses and physicochemical and biological studies of eight [$^{99\text{m}}\text{Tc}$]Tc(NS₃)(CN-NH(CH₂)_nTac) radioconjugates (Figure 3A)

consisting of ^{99m}Tc radionuclide coordinated by the tetradentate tripodal chelator (NS_3 , tris(2-mercaptoethyl)-amine) and a monodentate isocyanide ligand (CN-BFCA, succinimidyl isocyanobutyric ester) previously conjugated to the tacrine molecule (Tac) [33]. All radioconjugates turned out to be completely stable in a challenge experiment with cysteine and histidine solutions and in human serum. For the $[\text{}^{99m}\text{Tc}]\text{Tc}(\text{NS}_3)(\text{CN-NH}(\text{CH}_2)_7\text{Tac}$ radioconjugate characterized by the highest lipophilicity, stability tests in cerebrospinal fluid, biological activity towards acetylcholinesterase using Ellman's method and a multiorgan biodistribution study in normal mice were performed. For this radioconjugate and its parent tacrine-based complexing agent CN-NH(CH₂)₇Tac, computer docking studies were also performed. The biodistribution study showed a higher uptake of $[\text{}^{99m}\text{Tc}]\text{Tc}(\text{NS}_3)(\text{CN-NH}(\text{CH}_2)_7\text{Tac}$ in the liver than in the kidney, indicating the clearance of the radioconjugate mainly through the hepatic route. High uptake was also observed in the lung, but uptake in the brain was relatively low, nevertheless demonstrating the ability of the $[\text{}^{99m}\text{Tc}]\text{Tc}(\text{NS}_3)(\text{CN-NH}(\text{CH}_2)_7\text{Tac}$ radioconjugate to cross the blood–brain barrier.

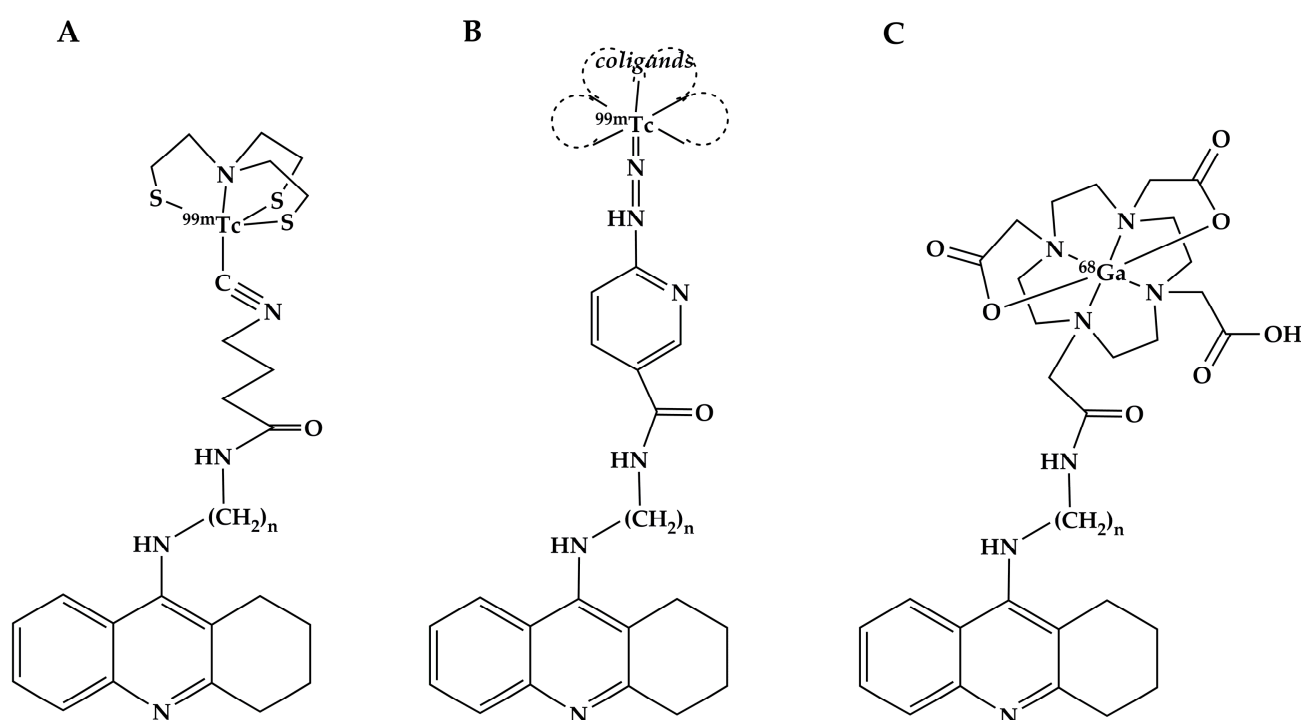


Figure 3. Radioconjugates based on tacrine derivatives: (A) $[\text{}^{99m}\text{Tc}]\text{Tc}(\text{NS}_3)(\text{CN-NH}(\text{CH}_2)_7\text{tacrine}$ [33]; (B) $[\text{}^{99m}\text{Tc}]\text{Tc-Hynic-(tricine)}_2\text{NH}(\text{CH}_2)_n\text{tacrine}$ [34]; (C) $[\text{}^{68}\text{Ga}]\text{Ga-DOTA-NH}(\text{CH}_2)_n\text{tacrine}$ [34].

Radioconjugates based on the same tacrine derivatives, containing the radionuclide ^{99m}Tc complexed by 6-hydrazinonicotinamide (HYNIC) and ^{68}Ga complexed by macrocyclic ligand 1,4,7,10-tetraazacyclododecane-1,4,7,10-tetraacetic acid (DOTA), are presented in another work by Gniazdowska et al. [34]. All synthesized $[\text{}^{99m}\text{Tc}]\text{Tc-Hynic-(tricine)}_2\text{NH}(\text{CH}_2)_n\text{tacrine}$ ($[\text{}^{99m}\text{Tc}]\text{Tc-Hynic-NH}(\text{CH}_2)_n\text{Tac}$) (Figure 3B), where n was in the range from two to nine, and $[\text{}^{68}\text{Ga}]\text{Ga-DOTA-NH}(\text{CH}_2)_n\text{tacrine}$ ($[\text{}^{68}\text{Ga}]\text{Ga-DOTA-NH}(\text{CH}_2)_n\text{Tac}$), where n was seven, eight or nine (Figure 3C), turned out to be completely stable in cysteine and histidine solutions (challenge experiments), in human serum and in cerebrospinal fluid. The lipophilicity parameter was determined for all radioconjugates, and the determined log D parameters showed that all $[\text{}^{99m}\text{Tc}]\text{Tc-Hynic-NH}(\text{CH}_2)_n\text{Tac}$ and $[\text{}^{68}\text{Ga}]\text{Ga-DOTA-NH}(\text{CH}_2)_n\text{Tac}$ radioconjugates are definitely hydrophilic compounds. Furthermore, the radioconjugates containing the $[\text{}^{68}\text{Ga}]\text{Ga-DOTA}$ complex were significantly more hydrophilic than the radioconjugates containing the $[\text{}^{99m}\text{Tc}]\text{Tc-Hynic}$ complex. For the two radioconjugates (one from each series, $[\text{}^{99m}\text{Tc}]\text{Tc-Hynic-NH}(\text{CH}_2)_9\text{Tac}$ and $[\text{}^{68}\text{Ga}]\text{Ga-DOTA-NH}(\text{CH}_2)_9\text{Tac}$, containing nine methylene CH_2 groups in the aliphatic chain) with

the most appropriate physicochemical properties (the highest possible lipophilicity parameter), cholinesterase inhibitory activity tests, biodistribution studies in mice and molecular modelling studies were carried out. Studies of the biological activity of the radioconjugates $[^{99m}\text{Tc}]\text{Tc-Hynic-NH}(\text{CH}_2)_9\text{Tac}$ and $[^{68}\text{Ga}]\text{Ga-DOTA-NH}(\text{CH}_2)_9\text{Tac}$ showed that these compounds have equally strong inhibitory properties against acetylcholinesterase (AChE) and butyrylcholinesterase (BuChE) as the reference compound tacrine. The *in vivo* biodistribution study showed the uptake of both radioconjugates in the brain, spleen, lungs, heart, kidneys and liver; however, the uptake of $[^{68}\text{Ga}]\text{Ga-DOTA-NH}(\text{CH}_2)_9\text{Tac}$ in the brain was very low. In general, the uptake of the $[^{99m}\text{Tc}]\text{Tc-Hynic-NH}(\text{CH}_2)_9\text{Tac}$ radioconjugate was significantly higher in all analyzed organs (its uptake in the brain was four times greater than that of the gallium radioconjugate). According to the authors, the low efficiency of crossing the blood–brain barrier of the tested radioconjugates may be due to their hydrophilic nature, and, for example, in the case of the gallium radioconjugates, the use of a chelator less hydrophilic than DOTA could increase the lipophilicity of the radioconjugate.

Studies on radioconjugates, still based on the same tacrine derivatives, in which five various chelators were used to complex the ^{68}Ga radionuclide, were presented in the work of Koźmiński et al. [35]. The chelators used for the synthesis of the ^{68}Ga -radioconjugates were 2,2'-(7-(1-carboxy-4-((2,5-dioxopyrrolidin-1-yl)oxy)-4-oxobutyl)-1,4,7-triazonane-1,4-diyl)diacetic acid (NODAGA-NHS), 2,2'-(7-(1-carboxy-4-((4-isothiocyanatobenzyl)amino)-4-oxobutyl)-1,4,7-triazonane-1,4-diyl)diacetic acid (NODAGA-Bn-NCS), 2,2',2''-(10-(1-carboxy-4-((4-isothiocyanatobenzyl)amino)-4-oxobutyl)-1,4,7,10-tetraazacyclododecane-1,4,7-triyl)triacetic acid (DOTAGA-Bn-NCS), [(R)-2-Amino-3-(4-isothiocyanatophenyl)propyl]-trans-(S,S)-cyclohexane-1,2-diamine-pentaacetic acid (DTPA-CHX-Bn-NCS) and N1,N7-bis((3-hydroxy-1,6-dimethyl-4-oxo-1,4-dihydropyridin-2-yl)methyl)-4-(3-(((3-hydroxy-1,6-dimethyl-4-oxo-1,4-dihydropyridin-2-yl)methyl)amino)-3-oxopropyl)-4-(3-(3-(4-isothiocyanatophenyl)thioureido)propanamido)heptanediamide (THP-Bn-NCS). In order to obtain the highest possible lipophilicity of the synthesized radioconjugates (recommended for radiopreparations capable of crossing the blood–tissue and blood–brain barriers), a tacrine derivative containing nine methylene groups in the aliphatic hydrocarbon chain was used for the synthesis of the ^{68}Ga -radioconjugates. All obtained radioconjugates (Figure 4) met the physicochemical properties required for radiopharmaceuticals. The tested inhibitory properties of the radioconjugates turned out to be no less than those of tacrine, which confirmed that the attachment of the radionuclide complex to tacrine through an appropriate linker does not change the biological properties of tacrine. Moreover, the $[^{68}\text{Ga}]\text{Ga-THP-NH}(\text{CH}_2)_9\text{Tac}$ radioconjugate showed a much stronger activity towards both AChE and BuChE than the parent tacrine compound. Lipophilicity tests showed that all newly synthesized radioconjugates were significantly less hydrophilic, and two of them, $[^{68}\text{Ga}]\text{Ga-NODAGA-Bn-NH}(\text{CH}_2)_9\text{Tac}$ and $[^{68}\text{Ga}]\text{Ga-THP-NH}(\text{CH}_2)_9\text{Tac}$, were already hydrophobic. These radioconjugates were selected for the biodistribution studies and molecular docking studies. The *in vivo* biodistribution studies in rats showed clearly different profiles. The $[^{68}\text{Ga}]\text{Ga-NODAGA-Bn-NH}(\text{CH}_2)_9\text{Tac}$ compound, apart from a relatively large accumulation in the excretory organs (kidneys and liver), accumulated in other organs (lungs, blood, heart and spleen) in small amounts. The compound $[^{68}\text{Ga}]\text{Ga-THP-NH}(\text{CH}_2)_9\text{Tac}$ circulated in the blood in large quantities and accumulated in comparable amounts in the excretory organs (kidneys, liver and spleen) as well as in the lungs and heart. Unfortunately, the uptake of both radioconjugates in the brain was low and insufficient from the point of view of potential application of these radioconjugates as a tool for the early diagnosis of Alzheimer's disease. Particularly noteworthy is the high uptake of the radioconjugate $[^{68}\text{Ga}]\text{Ga-THP-NH}(\text{CH}_2)_9\text{Tac}$ in the lungs, which indicates its specificity for this organ, and due to the presence of cholinesterase in the glial tissue of the lungs, it allows for the use of this radioconjugate as a tool for imaging pathological conditions of the lungs.

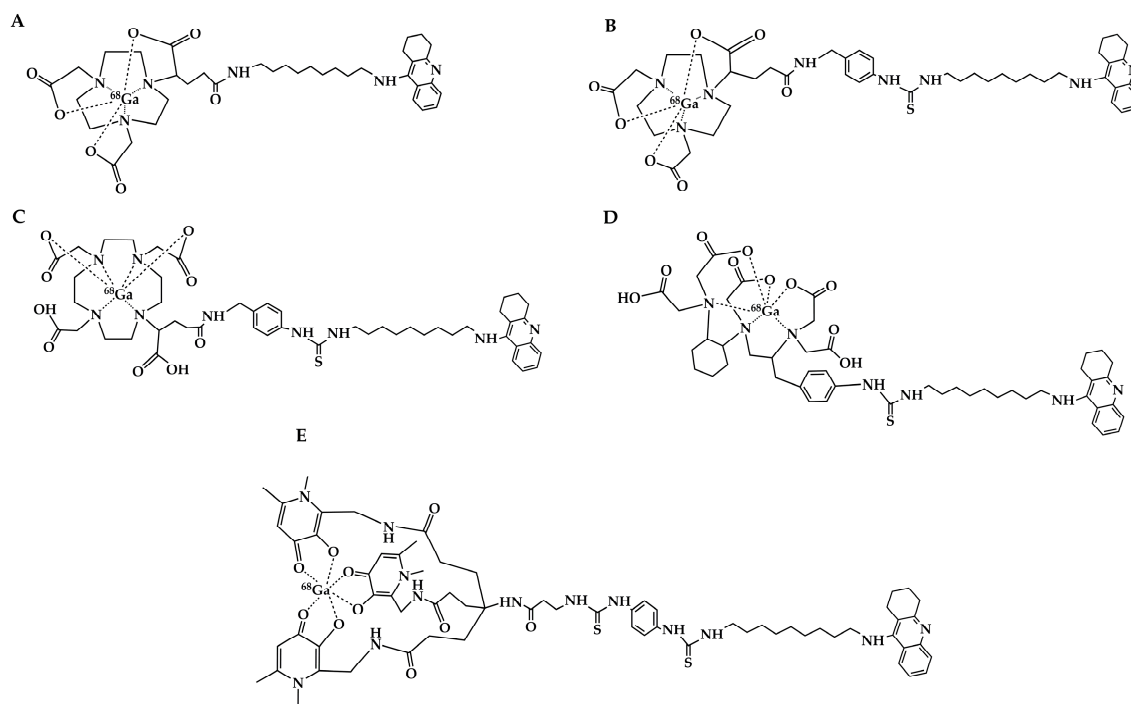


Figure 4. Radioconjugates based on tacrine derivatives [35]: (A) [^{68}Ga]Ga-NODAGA-NH(CH $_2$) $_9$ tacrine; (B) [^{68}Ga]Ga-NODAGA-Bn-NH(CH $_2$) $_9$ tacrine; (C) [^{68}Ga]Ga-DOTAGA-Bn-NH(CH $_2$) $_9$ tacrine; (D) [^{68}Ga]Ga-DTPA-CHX-NH(CH $_2$) $_9$ tacrine; (E) [^{68}Ga]Ga-THP-NH(CH $_2$) $_9$ tacrine.

In a review article focusing on potential radiotracers based on tacrine and its analogues, it is worth presenting the radioconjugates synthesized and tested by Szymański et al. [36]. Compared to previously used tacrine derivatives [33–35], the structural modification of tacrine additionally consisted of replacing the six-membered tetrahydroacridine ring with a five-membered ring. As previously reported [33–35], 6-hydrazinonicotinamide (HYNIC, radionuclide $^{99\text{m}}\text{Tc}$ complexing agent) was attached to the amino group of tacrine through a hydrocarbon chain with a different number of (CH $_2$) $_n$ groups, where $n = 2 \div 9$. Biochemical tests performed spectrophotometrically using the Ellman method showed that tacrine derivatives with the long hydrocarbon chain ($n = 7 \div 9$) have higher inhibition activity and are more selective towards acetylcholinesterase (AChE) than tacrine, while all compounds showed less selectivity for butyrylcholinesterase (BChE) compared to tacrine. The docking studies of the new tacrine derivatives to AChE and BChE showed that all tacrine derivatives bound to AChE in a similar way—they extended along the active gorge of the enzyme and interacted with the catalytic and peripheral sites. In the case of BChE, the binding method of the tacrine derivatives to the enzyme was similar with a slight difference regarding the location of the hydrazinonicotin fragment in the reduced peripheral anionic site of BChE. Among these tacrine derivatives, for the synthesis of the $^{99\text{m}}\text{Tc}$ -radioconjugate, the authors chose the derivative that contained two methylene groups in the hydrocarbon chain and was characterized by the highest activity towards BChE (the level of this enzyme varies in different stages of Alzheimer’s disease). The spectrophotometric test of this compound (6-Hydrazino-*N*-[2-(2,3-dihydro-1*H*-cyclopenta[*b*]quinolin-9-ylamino)Ethyl]nicotinamide) showed its stability in water. After labeling this compound with $^{99\text{m}}\text{Tc}$ radionuclide, the obtained radioconjugate [$^{99\text{m}}\text{Tc}$]Tc-Hynic-2,3-dihydro-1*H*-cyclopenta[*b*]quinolone (Figure 5) was used to study biodistribution in rats. The greatest accumulation of radioactivity was observed in the liver, followed by the kidneys, lungs and gastrointestinal tract. Unfortunately, the uptake of the radioconjugate in the brain was very low (probably due to the hydrophilic nature of the radioconjugate), which indicates that the tested radioconjugate does not have sufficient ability to cross the blood–brain barrier and cannot be considered as a potential agent in the diagnosis of Alzheimer’s disease.

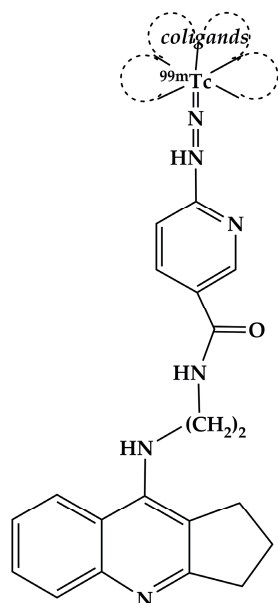


Figure 5. ^{99m}Tc -radioconjugate based on 2,3-dihydro-1H-cyclopenta[b]quinolone [36].

Concise information concerning radioconjugates based on tacrine derivatives is presented in Table 2.

Table 2. Radioconjugates based on tacrine derivatives.

Tacrine Derivative-Based Radioconjugates	Research Purpose and Conclusions	References
	Synthesis procedure	[26]
	<p>Studies in vivo in non-human primates: in rats (radioactivity was measured in blood, plasma, heart, liver, kidneys, lungs, skeletal muscles and brain (separately in the pons, cerebellum, colliculi, hypothalamus, hippocampus, striatum and anterior and posterior cortices)), and PET imaging on two male adult baboons using both $^{[11]\text{C}}\text{MTHA}$ radiotracer alone and $^{[11]\text{C}}\text{MTHA}$ radiotracer together with unlabeled THA</p> <ul style="list-style-type: none"> • Radioactivity accumulated in all brain regions studied; in the case of co-injection of THA together with $^{[11]\text{C}}\text{MTHA}$, accumulation was significantly lower; • These two molecules, $^{[11]\text{C}}\text{MTHA}$ and THA, compete for the same binding sites; • The $^{[11]\text{C}}\text{MTHA}$ radiotracer could be considered a promising PET ligand for studying THA binding in the brain. 	[27]
$^{[11]\text{C}}\text{MTHA}$	<p>Studies in vivo in healthy human volunteers and measurement of radioactivity accumulated in all brain regions studied in the case of co-injection of THA together with $^{[11]\text{C}}\text{MTHA}$</p> <ul style="list-style-type: none"> • Determined radioactivity in the brain was relatively high and amounted to approximately 6% of the administered dose; • Brain accumulation of the radiotracer $^{[11]\text{C}}\text{MTHA}$ differs from the sites of action and/or sites of elevated AChE concentrations detected post-mortem in human brains; • Cerebral distribution of the $^{[11]\text{C}}\text{MTHA}$ radiotracer in the human nervous system is not parallel with AChE, so the clinical effect of THA may also occur in a way other than through the cholinergic neuronal system. 	[28]

Table 2. Cont.

Tacrine Derivative-Based Radioconjugates	Research Purpose and Conclusions	References
9-amino-8-fluoro-2,4-methane-1,2,3,4-[9- ¹⁴ C]tetrahydroacridine	Synthesis procedure of radiopreparation dedicated for metabolic studies, potential therapeutic radiopharmaceutical in AD	[29]
[¹²³ I]7-I-THA	Procedure for the synthesis of a potential agent for imaging the map of acetylcholinesterase (AChE) receptor sites in living organisms	[30]
[^{99m} Tc]Tc(NS ₃)(CN-NH(CH ₂) _n Tac	<p>Synthesis and physicochemical properties of radioconjugates, multiorgan biodistribution study of [^{99m}Tc]Tc(NS₃)(CN-NH(CH₂)₇Tac in normal mice, computer docking studies of [^{99m}Tc]Tc(NS₃)(CN-NH(CH₂)₇Tac and its parent tacrine-based complexing agent CN-NH(CH₂)₇Tac</p> <ul style="list-style-type: none"> • A higher uptake in liver than in kidney indicates the clearance of the radioconjugate mainly through the hepatic route; • A high uptake in the lung and relatively low uptake in the brain 	[33]
[^{99m} Tc]Tc-Hynic-NH(CH ₂) _n Tac, [68Ga]Ga-DOTA-NH(CH ₂) _n Tac	<p>Synthesis and physicochemical properties of radioconjugates, biodistribution studies in mice and molecular modelling studies of [^{99m}Tc]Tc-Hynic-NH(CH₂)₉Tac and [68Ga]Ga-DOTA-NH(CH₂)₉Tac</p> <ul style="list-style-type: none"> • Radioconjugates containing the [68Ga]Ga-DOTA complex are significantly more hydrophilic than radioconjugates containing the [^{99m}Tc]Tc-Hynic complex; • The uptake of the [^{99m}Tc]Tc-Hynic-NH(CH₂)₉Tac radioconjugate was significantly higher in all analyzed organs than that of [68Ga]Ga-DOTA-NH(CH₂)₉Tac. 	[34]
[68Ga]Ga-NODAGA-NH(CH ₂) ₉ Tac, [68Ga]Ga-NODAGA-Bn-NH(CH ₂) ₉ Tac, [68Ga]Ga-DOTAGA-Bn-NH(CH ₂) ₉ Tac, [68Ga]Ga-DTPA-CHX-NH(CH ₂) ₉ Tac, [68Ga]Ga-THP-NH(CH ₂) ₉ Tac	<p>Synthesis and physicochemical properties of ⁶⁸Ga-radioconjugates using the five various chelators NODAGA-NHS, NODAGA-Bn-NCS, DOTAGA-Bn-NCS, DTPA-CHX-Bn-NCS-THP-Bn-NCS, biodistribution studies in mice and molecular modelling studies of [68Ga]Ga-NODAGA-Bn-NH(CH₂)₉Tac and [68Ga]Ga-THP-NH(CH₂)₉Tac</p> <ul style="list-style-type: none"> • Radioconjugates [68Ga]Ga-NODAGA-NH(CH₂)₉Tac, [68Ga]Ga-DOTAGA-Bn-NH(CH₂)₉Tac and [68Ga]Ga-DTPA-CHX-NH(CH₂)₉Tac were hydrophilic; • [68Ga]Ga-NODAGA-Bn-NH(CH₂)₉Tac and [68Ga]Ga-THP-NH(CH₂)₉Tac were hydrophobic; • The uptake of the [68Ga]Ga-NODAGA-Bn-NH(CH₂)₉Tac and [68Ga]Ga-THP-NH(CH₂)₉Tac radioconjugates in the brain was low and insufficient from the point of view of their application for the early diagnosis of AD; • Relatively high uptake of [68Ga]Ga-THP-NH(CH₂)₉Tac in the lungs. 	[35]
[^{99m} Tc]Tc-Hynic-(CH ₂) ₂ ,2,3-dihydro-1H-cyclopenta[b]quinolone	<p>Synthesis, physicochemical properties and docking studies of Hynic-(CH₂)_n-2,3-dihydro-1H-cyclopenta[b]quinolone derivatives, synthesis, physicochemical properties and biodistribution studies in rats of [^{99m}Tc]Tc-Hynic-(CH₂)₂-2,3-dihydro-1H-cyclopenta[b]quinolone radioconjugate</p> <ul style="list-style-type: none"> • Derivative containing two methylene groups in the hydrocarbon chain was characterized by the highest activity towards BChE; • The highest uptake of radioconjugate was observed in the liver, followed by the kidneys, lungs and gastrointestinal tract; • Low uptake of the radioconjugate in the brain. 	[36]

2.3. Molecular Modeling Studies of Tacrine Derivatives—Cholinesterase Interaction

The study of the crystal structure of *Torpedo californica* acetylcholinesterase (TcAChE) made possible, for the first time at atomic resolution, the visualization of the acetylcholine (ACh) binding pocket [37–39]. The binding pocket is a narrow and deep gorge approximately 5 Å wide and 20 Å long and lined (in approximately 40–60%) with rings of 14 conserved aromatic residues: Y70, W84, F120, Y121, Y130, W233, W279, F288, F290, F330, F331, Y334, W432 and Y442 [28]. It penetrates into the enzyme more than halfway and expands near the bottom to form a cavity called the active binding site, containing the catalytic triad S200, E327 and H440 (Figure 7 in ref. [37]). Five amino acids, Tyr70, Asp72, Tyr121, Trp279 and Tyr334, located at the entrance to the gorge, constitute the peripheral anionic site (PAS) binding for AChE [38]. A large number of aromatic residues in the gorge walls and bases in the gorge bottom result in many different hydrophobic and “anionic” interaction sites in the binding pocket, located separately or overlapping with the active sites of the ACh-binding enzyme (the ACh binding site in AChE contains from six to nine negative charges). The aromatic nature of the gorge influences the high degree of binding of a given substrate and thus the high catalytic activity of the enzyme. TcAChE has a very large dipole moment, which is greatly influenced by the presence of five acidic amino acids located around the entrance to the gorge. The axis of the AChE dipole moment is oriented along the axis of the gorge’s active sites. Along the gorge, along the entire length of the active sites, there is a potential gradient that can effectively pull the substrate appearing at the gorge mouth (Y121, F330) down the gorge.

Computational studies of the interaction of some tacrine derivatives as well as potential radiotracers based on them (Table 3) with acetyl- and/or butyrylcholinesterase were discussed in the works of Gniazdowska et al. [33,34], Koźmiński et al. [35] and Szymański et al. [36]. The conjugates and radioconjugates selected for the molecular docking studies are listed in Table 3.

Table 3. List and structure of conjugates and radioconjugates selected for research using computer calculations.

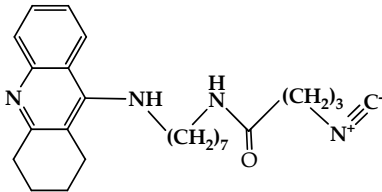
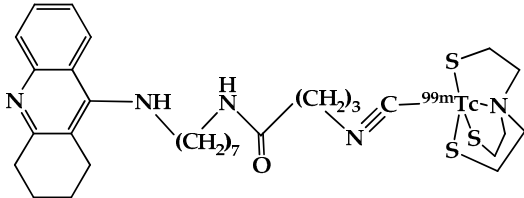
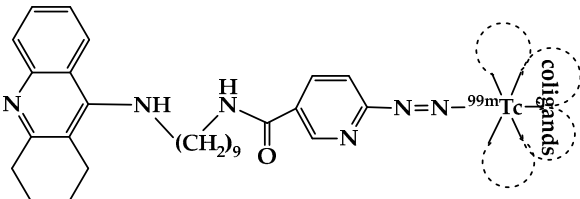
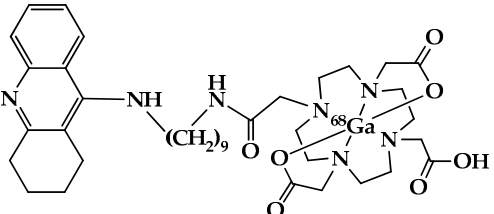
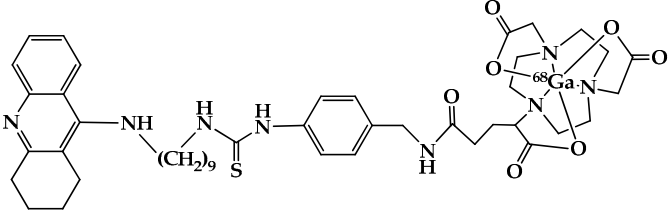
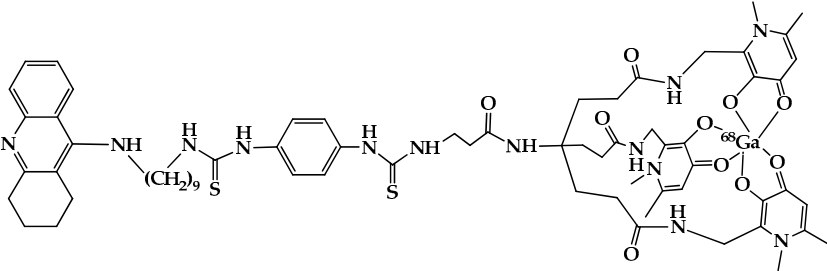
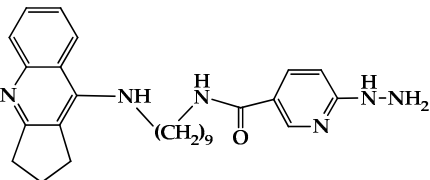
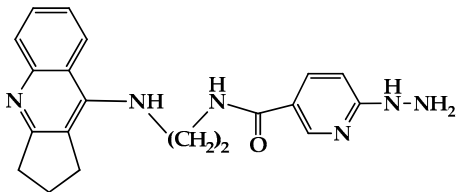
Radio(conjugates)	Molecular Docking Studies to	
	AChE [Ref.]	BChE [Ref.]
	Figure 5 in [33]	----
	Figure 5 in [33]	----
	Figure 7 in [34]	----

Table 3. Cont.

Radio(conjugates)	Molecular Docking Studies to	
	AChE [Ref.]	BChE [Ref.]
	-----	Figure 8 in [34]
	Figure 8 in [35]	-----
	Figure 8 in [35]	-----
	Figure 1 in [36]	-----
	-----	Figure 2 in [36]

Molecular modeling studies made it possible to determine the structure of the inhibitor–cholinesterase system and to determine and locate individual interactions between the components of this system responsible for the action of the inhibitor on the enzyme. Detailed information about the nature and location of individual interactions of the inhibitor with the amino acids forming the enzyme’s binding pocket is provided in the cited publications.

In general, all tested inhibitors had similar components, namely tacrine, a longer or shorter linker in the form of a hydrocarbon chain and, optionally, a radionuclide complex. Therefore, their fit into the cholinesterase binding pocket and their interactions with AChE and BChE were similar. A fragment of tacrine (as well as a tacrine analog with a cyclopentane ring) was located at the bottom of the gorge, and the main interaction here was the interaction with the catalytic triad. The hydrocarbon chain was located along the gorge and formed hydrophobic interactions with the aromatic rings of the amino acids present in

the gorge wall. The radionuclide complex is usually located outside or at the entry to the gorge of the binding pocket and interacted through peripheral anionic sites.

3. Discussion

The works discussed in this article focused on the search for a diagnostic radiopharmaceutical for the earliest possible diagnosis of Alzheimer's disease. The biologically active molecule in these radiopharmaceuticals was the medicinal preparation tacrine (or its derivatives) that was approved by the FDA in 1993 for the treatment of Alzheimer's disease and was, in 2013, withdrawn due to harmful side effects. However, since radiopharmaceuticals are administered to the patient in microgram quantities and, in the case of diagnostic radiopharmaceuticals, their use is not frequent, the problem of the harmfulness of tacrine is not significant. However, due to the high ability of tacrine to cross the blood–brain barrier, its use as a vector in radiopharmaceuticals is justified.

As can be observed from the presented works, radiotracers based on the tacrine molecule, in which the radionuclide (^3H , ^{11}C , ^{14}C) is an isotope of one of the elements included in the tacrine molecule [9–12], easily cross the blood–brain barrier and accumulate in significant amounts in the brain. However, such radiopreparations are not easily available due to the too complicated procedures for synthesizing these radiopreparations, which are difficult or even impossible to perform in clinical conditions (in hospital laboratories).

The procedures for obtaining radioconjugates in the form of a tacrine solution, tacrine microemulsion and tacrine mucoadhesive microemulsion labeled (directly) with $^{99\text{m}}\text{Tc}$ and identifying them using the radio-TLC method [24,25] are relatively easy and can be performed in hospital laboratories. These radiopreparations accumulated relatively well in the brain, but regarding these compounds, there is no knowledge about their composition and structure, which, according to the authors of this review article, is a significant disadvantage. For these radiopreparations, intranasal administration has proven to be more effective than intravenous administration.

Radiopreparations based on a relatively minimally changed tacrine molecule also accumulated satisfactorily in the brain [26–30]. Modification of tacrine by adding a methyl group, fluorine or iodine did not reduce the ability of tacrine to cross the blood–brain barrier.

The most convenient procedure for the synthesis of diagnostic radiopharmaceuticals in clinical conditions is to perform a labeling reaction with generator radionuclides ($^{99\text{m}}\text{Tc}$, ^{68}Ga) of the active substance (tacrine or its derivative, often previously coupled with an appropriate chelator) included in the so-called kit [33–36] (kits are ready-made sets containing, in lyophilized form, the appropriate reagents in the appropriate quantities needed for the synthesis of a given radiopharmaceutical). However, the use of chelators significantly changes both the size of the final radiopreparation and its lipophilicity. Changes in these parameters do not have a significant impact on the inhibitory properties towards acetyl- and butyrylcholinesterase, but their effect *in vivo* is a significant reduction in the ability of the radiopharmaceutical to cross the blood–brain barrier and accumulate in the brain in the amounts necessary for imaging.

To sum up, it can be said that, despite many works, it has not been possible to find a radiopreparation based on tacrine or its derivatives that meets the requirements for radiopharmaceuticals. Perhaps it would be advisable to search for another biological molecule involved in the course of Alzheimer's disease from its earliest stage.

Author Contributions: Conceptualization, E.G. and P.K.; writing—original draft preparation, E.G. and P.K.; writing—review and editing, E.G. and P.K.; visualization, E.G. and P.K.; supervision, E.G.; project administration, E.G. and P.K. All authors have read and agreed to the published version of the manuscript.

Funding: This research received no external funding. This work has been supported by the statutory activity of the Institute of Nuclear Chemistry and Technology, Warsaw, Poland.

Institutional Review Board Statement: Not applicable.

Informed Consent Statement: Not applicable.

Data Availability Statement: No new data were created or analyzed in this study. Data sharing is not applicable to this article.

Conflicts of Interest: The authors declare no conflicts of interest.

Abbreviations

AChE	acetylcholinesterase
AD	Alzheimer's disease
APP	amyloid precursor protein
BChE, BuChE	butyrylcholinesterase
BFCA	bifunctional coupling agent
CN-BFCA	succinimidyl isocyanobutyric ester
CNS	central nervous system
DOTA	1,4,7,10-tetraazacyclododecane-1,4,7,10-tetraacetic acid
DOTAGA-Bn-NCS	2,2',2''-(10-(1-carboxy-4-((4-isothiocyanatobenzyl)amino)-4-oxobutyl)-1,4,7,10-tetraazacyclododecane-1,4,7-triyl)triacetic acid
DTPA-CHX-Bn-NCS	[(R)-2-Amino-3-(4-isothiocyanatophenyl)propyl]-trans-(S,S)-cyclohexane-1,2-diamine-pentaacetic acid
FDA	US Food and Drug Administration
HYNIC	6-hydrazinonicotinamide
IN	intranasal
IR	infrared spectrum
IV	intravenous
MRI	magnetic resonance imaging
MS	mass spectrum
MTHA, N-methyl-THA	1,2,3,4-tetrahydro-9-methyl-amino acridine
NMR	nuclear magnetic resonance
NODAGA-Bn-NCS	2,2'-(7-(1-carboxy-4-((4-isothiocyanatobenzyl)amino)-4-oxobutyl)-1,4,7-triazonane-1,4-diyl)diacetic acid
NODAGA-NHS	2,2'-(7-(1-carboxy-4-((2,5-dioxopyrrolidin-1-yl)oxy)-4-oxobutyl)-1,4,7-triazonane-1,4-diyl)diacetic acid
NS ₃	tris(2-mercaptoethyl)-amine
PET	positron emission tomography
RHPLC	radio-high performance liquid chromatography
RTLC	radio-thin layer chromatography
SPECT	single photon emission computer tomography
THA, Tac	1,2,3,4-tetrahydro-9-amino acridine
THP-Bn-NCS	N1,N7-bis((3-hydroxy-1,6-dimethyl-4-oxo-1,4-dihydropyridin-2-yl)methyl)-4-(3-(((3-hydroxy-1,6-dimethyl-4-oxo-1,4-dihydropyridin-2-yl)methyl)amino)-3-oxopropyl)-4-(3-(3-(4-isothiocyanatophenyl)thioureido)propanamido)heptanediamide
TLC	thin-layer chromatography
TME	tacrine microemulsion
TMME	tacrine mucoadhesive microemulsion
TS	tacrine solution

References

1. Mikiciuk-Olasik, E.; Szymański, P.; Żurek, E. Diagnostics and therapy of Alzheimer's disease. *Indian J. Exp. Biol.* **2007**, *45*, 315–325. [[PubMed](#)]
2. Declercq, L.D.; Vandenberghe, R.; Van Laere, K.; Verbruggen, A.; Bormans, G. Drug Development in Alzheimer's Disease: The Contribution of PET and SPECT. *Front. Pharmacol.* **2016**, *7*, 88. [[CrossRef](#)] [[PubMed](#)]
3. Knopman, D.S.; Amieva, H.; Petersen, R.C.; Chételat, G.; Holtzman, D.M.; Hyman, B.T.; Nixon, R.A.; Jones, D.T. Alzheimer disease. *Nat. Rev. Dis. Primers* **2021**, *7*, 33. [[CrossRef](#)] [[PubMed](#)]
4. Long, J.M.; Holtzman, D.M. Alzheimer Disease: An Update on Pathobiology and Treatment Strategies. *Cell* **2019**, *179*, 312–339. [[CrossRef](#)] [[PubMed](#)]

5. Sienski, G.; Narayan, P.; Bonner, J.M.; Kory, N.; Boland, S.; Arczewska, A.A.; Ralvenius, W.T.; Akay, L.; Lockshin, E.; He, L.; et al. APOE4 disrupts intracellular lipid homeostasis in human iPSC-derived glia. *Sci. Transl. Med.* **2021**, *13*, eaaz4564. [[CrossRef](#)] [[PubMed](#)]
6. Tackenberg, C.; Kulic, L.; Nitsch, R.M. Familial Alzheimer's disease mutations at position 22 of the amyloid β -peptide sequence differentially affect synaptic loss, tau phosphorylation and neuronal cell death in an ex vivo system. *PLoS ONE* **2020**, *15*, e0239584. [[CrossRef](#)] [[PubMed](#)]
7. Chen, Z.R.; Huang, J.B.; Yang, S.L.; Hong, F.F. Role of Cholinergic Signaling in Alzheimer's Disease. *Molecules* **2022**, *27*, 1816. [[CrossRef](#)] [[PubMed](#)]
8. Francis, P.; Palmer, A.; Snape, M. The cholinergic hypothesis of Alzheimer's disease: A review of progress. *J. Neurol. Neurosurg. Psychiatry* **1999**, *66*, 137–147. [[CrossRef](#)] [[PubMed](#)]
9. Camps, P.; Munoz-Torrero, D. Cholinergic drugs in pharmacotherapy of Alzheimer's disease. *Mini Rev. Med. Chem.* **2002**, *2*, 11–25. [[CrossRef](#)]
10. Ferreira-Vieira, T.H.; Guimaraes, I.M.; Silva, F.R.; Ribeiro, F.M. Alzheimer's disease: Targeting the Cholinergic System. *Curr. Neuropharmacol.* **2016**, *14*, 101–115. [[CrossRef](#)]
11. Colović, M.B.; Krstić, D.Z.; Lazarević-Pašti, T.D.; Bondžić, A.M.; Vasić, V.M. Acetylcholinesterase inhibitors: Pharmacology and toxicology. *Curr. Neuropharmacol.* **2013**, *11*, 315–335. [[CrossRef](#)] [[PubMed](#)]
12. Walczak-Nowicka, L.J.; Herbert, M. Acetylcholinesterase Inhibitors in the Treatment of Neurodegenerative Diseases and the Role of Acetylcholinesterase in their Pathogenesis. *Int. J. Mol. Sci.* **2021**, *22*, 9290. [[CrossRef](#)]
13. Ruangritchankul, S.; Chantharit, P.; Srisuma, S.; Gray, L.C. Adverse Drug Reactions of Acetylcholinesterase Inhibitors in Older People Living with Dementia: A Comprehensive Literature Review. *Ther. Clin. Risk Manag.* **2021**, *17*, 927–949. [[CrossRef](#)] [[PubMed](#)]
14. Jann, M.W.; Shirley, K.L.; Small, G.W. Clinical pharmacokinetics and pharmacodynamics of cholinesterase inhibitors. *Clin. Pharmacokinet.* **2002**, *41*, 719–739. [[CrossRef](#)]
15. Crismon, M.L. Tacrine: First drug approved for Alzheimer's disease. *Ann. Pharmacother.* **1994**, *28*, 744–751. [[CrossRef](#)] [[PubMed](#)]
16. Riekkinen, P., Jr.; Kuikka, J.; Soininen, H.; Helkala, E.L.; Hallikainen, M.; Riekkinen, P. Tetrahydroaminoacridine modulates technetium-99m labelled ethylene dicysteinat retention in Alzheimer's disease measured with single photon emission computed tomography imaging. *Neurosci. Lett.* **1995**, *195*, 53–56. [[CrossRef](#)]
17. Stanciu, G.D.; Luca, A.; Rusu, R.N.; Bild, V.; Beschea Chiriac, S.I.; Solcan, C.; Bild, W.; Ababei, D.C. Alzheimer's Disease Pharmacotherapy in Relation to Cholinergic System Involvement. *Biomolecules* **2020**, *10*, 40. [[CrossRef](#)]
18. Holden, M.; Kelly, C. Use of cholinesterase inhibitors in dementia. *Adv. Psychiatr. Treat.* **2002**, *8*, 89–96. [[CrossRef](#)]
19. Mimica, N.; Presečki, P. Side Effects of Approved Antidementives. *Psychiatr. Danub.* **2009**, *21*, 108–113.
20. McNally, W.; Roth, M.; Young, R.; Bockbrader, H.; Chang, T. Quantitative whole-body autoradiographic determination of tacrine tissue distribution in rats following intravenous or oral dose. *Pharm. Res.* **1989**, *6*, 924–930. [[CrossRef](#)]
21. McNally, W.; Pool, W.F.; Sinz, M.W.; Dehart, P.; Ortwine, D.F.; Huang, C.C.; Chang, T.; Woolf, T.F. Distribution of tacrine and metabolites in rat brain and plasma after single- and multiple-dose regimens. Evidence for accumulation of tacrine in brain tissue. *Drug Metab. Dispos.* **1996**, *24*, 628–633. [[PubMed](#)]
22. Mena, E.E.; Desai, M.C. High-affinity [^3H]THA (tetrahydroaminoacridine) binding sites in rat brain. *Pharm. Res.* **1991**, *8*, 200–203. [[CrossRef](#)]
23. Egan, J.A.; Nugent, R.P.; Filer, C.N. Tritium labelling and characterization of the cognition enhancing drug tacrine using several precursors. *Appl. Radiat. Isot.* **2002**, *57*, 837–840. [[CrossRef](#)] [[PubMed](#)]
24. Jogani, V.V.; Shah, P.J.; Mishra, P.; Mishra, A.K.; Misra, A.R. Nose-to-brain delivery of tacrine. *J. Pharm. Pharmacol.* **2007**, *59*, 1199–1205. [[CrossRef](#)]
25. Jogani, V.V.; Shah, P.J.; Mishra, P.; Mishra, A.K.; Misra, A.R. Intranasal mucoadhesive microemulsion of tacrine to improve brain targeting. *Alzheimer Dis. Assoc. Disord.* **2008**, *22*, 116–124. [[CrossRef](#)] [[PubMed](#)]
26. Bonnot, S.; Prenant, C.; Crouzel, C. Synthesis of 9-[^{11}C]methylamino-1,2,3,4-tetrahydroacridine, a potent acetylcholine esterase inhibitor. *Appl. Radiat. Isot.* **1991**, *42*, 690–691. [[CrossRef](#)]
27. Tavitian, B.; Pappata, S.; Bonnot-Lours, S.; Prenant, C.; Jobert, A.; Crouzel, C.; Di Giamberardino, L. Positron emission tomography study of [^{11}C]methyl-tetrahydroaminoacridine (methyl-tacrine) in baboon brain. *Eur. J. Pharmacol.* **1993**, *236*, 229–238. [[CrossRef](#)] [[PubMed](#)]
28. Traykov, L.; Tavitian, B.; Jobert, A.; Boller, F.; Forette, F.; Crouzel, C.; Di Giamberardino, L.; Pappata, S. In vivo PET study of cerebral [^{11}C] methyl- tetrahydroaminoacridine distribution and kinetics in healthy human subjects. *Eur. J. Neurol.* **1999**, *6*, 273–278. [[CrossRef](#)]
29. Nishioka, K.; Kamada, T.; Kanamaru, H. ^{14}C -labeling of a tetrahydroacridine, a novel CNS-selective cholinesterase inhibitor. *J. Label. Compd. Radiopharm.* **1992**, *31*, 553–560. [[CrossRef](#)]
30. Akula, M.R.; Kabalka, G.W. Synthesis of 7-[^{123}I]iodotacrine: A potential SPECT agent to map acetylcholinesterase. *J. Label. Compd. Radiopharm.* **1999**, *42*, 959–964. [[CrossRef](#)]
31. Szymański, P.; Zurek, E.; Mikiciuk-Olasik, E. New tacrine-hydrazinonicotinamide hybrids as acetylcholinesterase inhibitors of potential interest for the early diagnostics of Alzheimer's disease. *Pharmazie* **2006**, *61*, 269–273. [[CrossRef](#)]

32. Szymański, P.; Markowicz, M.; Mikiciuk-Olasik, E. Synthesis and biological activity of derivatives of tetrahydroacridine as acetylcholinesterase inhibitors. *Bioorg. Chem.* **2011**, *39*, 138–142. [[CrossRef](#)] [[PubMed](#)]
33. Gniazdowska, E.; Koźmiński, P.; Wasek, M.; Bajda, M.; Sikora, J.; Mikiciuk-Olasik, E.; Szymański, P. Synthesis, physicochemical and biological studies of technetium-99m labeled tacrine derivative as a diagnostic tool for evaluation of cholinesterase level. *Bioorg. Med. Chem.* **2017**, *25*, 912–920. [[CrossRef](#)] [[PubMed](#)]
34. Gniazdowska, E.; Koźmiński, P.; Halik, P.; Bajda, M.; Czarnecka, K.; Mikiciuk-Olasik, E.; Masłowska, K.; Rogulski, Z.; Cheda, Ł.; Kilian, K.; et al. Synthesis, physicochemical and biological evaluation of tacrine derivative labeled with technetium-99m and gallium-68 as a prospective diagnostic tool for early diagnosis of Alzheimer's disease. *Bioorg. Chem.* **2019**, *91*, 103136. [[CrossRef](#)] [[PubMed](#)]
35. Koźmiński, P.; Niedziałek, D.; Wieczorek, G.; Halik, P.K.; Czarnecka, K.; Rogut, A.; Cheda, Ł.; Rogulski, Z.; Szymański, P.; Gniazdowska, E. New Imaging Modality of COVID-19 Pneumonia Developed on the Basis of Alzheimer's Disease Research. *Int. J. Mol. Sci.* **2022**, *23*, 8405. [[CrossRef](#)] [[PubMed](#)]
36. Szymański, P.; Lázníčková, A.; Lázníček, M.; Bajda, M.; Malawska, B.; Markowicz, M.; Mikiciuk-Olasik, E. 2,3-dihydro-1H-cyclopenta[b]quinoline derivatives as acetylcholinesterase inhibitors-synthesis, radiolabeling and biodistribution. *Int. J. Mol. Sci.* **2012**, *13*, 10067–10090. [[CrossRef](#)] [[PubMed](#)]
37. Dvir, H.; Silman, I.; Harel, M.; Rosenberry, T.L.; Sussman, J.L. Acetylcholinesterase: From 3D structure to function. *Chem. Biol. Interact.* **2010**, *187*, 10–22. [[CrossRef](#)] [[PubMed](#)]
38. Bajda, M.; Więckowska, A.; Hebda, M.; Guzior, N.; Sottriffer, C.A.; Malawska, B. Structure-Based Search for New Inhibitors of Cholinesterases. *Int. J. Mol. Sci.* **2013**, *14*, 5608–5632. [[CrossRef](#)]
39. Xu, Y.; Cheng, S.; Sussman, J.L.; Silman, I.; Jiang, H. Computational Studies on Acetylcholinesterases. *Molecules* **2017**, *22*, 1324. [[CrossRef](#)]

Disclaimer/Publisher's Note: The statements, opinions and data contained in all publications are solely those of the individual author(s) and contributor(s) and not of MDPI and/or the editor(s). MDPI and/or the editor(s) disclaim responsibility for any injury to people or property resulting from any ideas, methods, instructions or products referred to in the content.